ANALYSIS OF MECHANICAL IMPACT ON CERAMIC TILE. INFLUENCING FACTORS

V. Cantavella[(1)], A. Moreno[(1)], C. Felíu[(1)], A. Muñoz[(1)], J. Barberá[(2)], A. Palanques[(2)]

[(1)] Instituto de Tecnología Cerámica (ITC). Asociación de Investigación de las Industrias Cerámicas (AICE)
Universitat Jaume I. Castellón. Spain.
[(2)] Cerámica Saloni, S.A. San Juan de Moró. Spain.

ABSTRACT

One of the fields in which ceramic materials usually display worse behaviour is that of impact resistance. With a view to better understanding the mechanisms that lead to rupture during impact, as well as to establishing the factors that influence rupture, finite element modelling was performed of the impact of a rigid object on a glazed tile. The results showed that stresses developed solely in the area close to contact. In addition, the development of damage during impact depended on the maximum stress at the point of impact, and was not very sensitive to the speed at which this load was applied.

The similarity of the damage produced in dynamic and quasi-static impacts has allowed development of a procedure for quantifying impact resistance, based on the application of a cyclical load on a tile by means of an indenter and the measurement of penetration depth as a function of the number of cycles.

Finally, the effect has been analysed of certain factors on the damage produced during impact.

1. INTRODUCTION

Ceramic materials, and tiles in particular, display brittle behaviour, which becomes evident in the case of mechanical stresses associated with impact by falling objects.

A series of tensions develop during impact, which change with time. These tensions produce shear, tensile, and compression stresses that may ultimately lead to spalling at the point of impact.

Current standards simply evaluate impact resistance by using the coefficient of restitution[1], which measures the quotient between the start and end heights of a ball that is dropped on to the tile. This parameter exhibits little variation from one type of tile to another, while it is very sensitive to the way the tile is fixed.

More rigorous methods have been developed to measure impact resistance[2.3.4]; however, a literature survey found no studies that analysed the stresses that developed at the moment of impact. Knowledge of these stresses could help better understand the processes that cause rupture during impact.

2. MODELLING OF THE IMPACT

2.1. DYNAMIC IMPACT

2.1.1. Description of the model

In order to model the impact, a tile made up of three elastic sheets was considered: substrate, engobe, and glaze. The tile was set on a mortar layer, which was also considered elastic (Figure 1).

The impinging element was a dart (indenter), consisting of a semi-spherical tip, joined to the end of a cylinder that provided a given inertia to the assembly. Owing to the axial symmetry of the problem, only a cross-section of the tile/dart ensemble was simulated, which allowed the original problem to be reduced from 3D to 2D.

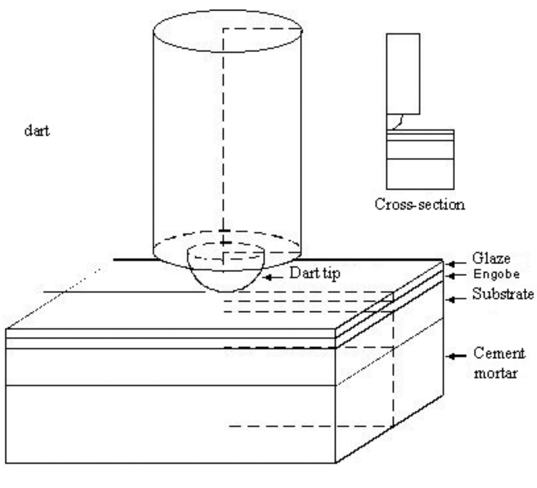

Figure 1. Scheme of the dart and the tile used in the finite element calculation. Owing to the axial symmetry, only one cross-section has been modelled

The calculation was carried out using the finite element method, which basically consists of dividing the solid (both the dart and the tile) into a series of cells, termed elements, and calculating the solution at the element nodes. The software program used was Code_Aster[5], distributed by EDF under an open code license.

Figure 2 shows the mesh used and Figure 3 presents a mesh detail near the contact point. The two top rows of quadrilaterals of the tile correspond to the glaze, and the following two to the engobe. The substrate and the bottom layer are meshed with triangles, element density increasing near the contact point with the dart.

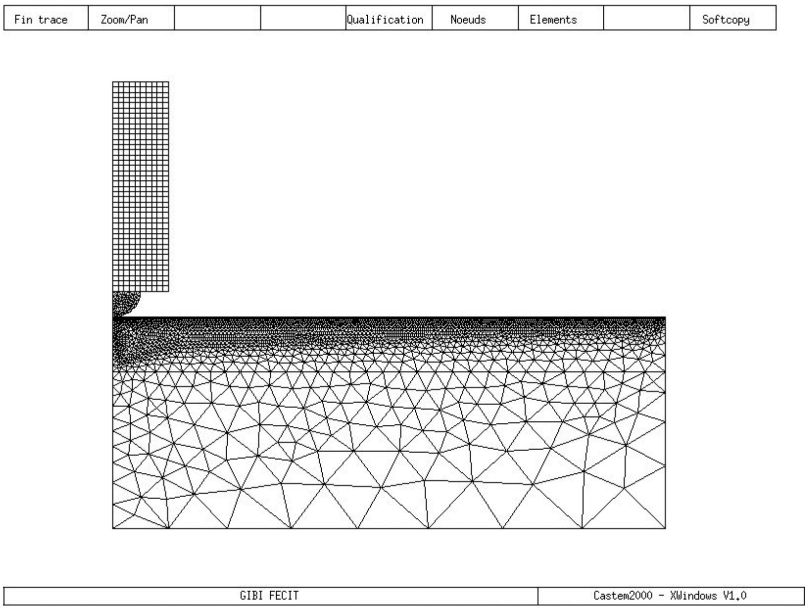

Figure 2. Meshing used in the finite element calculation.

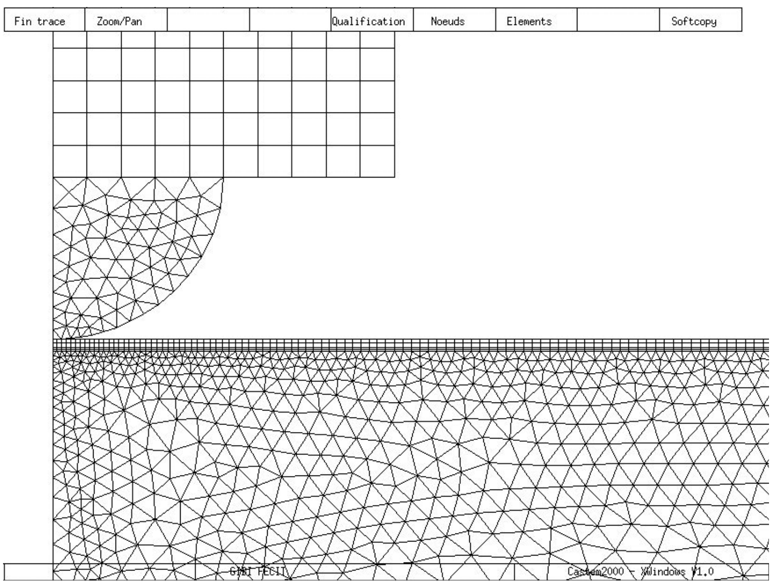

Figure 3. Meshing used in the finite element calculation.

2.1.2. *Results of the simulation*

The following parameters were used to carry out the simulation:

Impacting element (dart):

Dart tip radius: 5 mm

Dart length: 45 mm

Modulus of elasticity (steel): 210 GPa

Poisson's ratio: 0.25

Mass: 100 g

Drop height: 0.8 m

Ceramic tile:

Substrate thickness: 10 mm

Substrate modulus of elasticity: 30 GPa

Engobe thickness: 125 μm

Engobe modulus of elasticity: 30 GPa

Glaze thickness: 250 μm

Glaze modulus of elasticity glaze: 75 GPa

Poisson's ratio [generic for all layers]: 0.23

Fixing:

Thickness of the cement mortar or regulating layer: 30 mm

Cement modulus of elasticity: 20 GPa

Poisson's ratio: 0.20

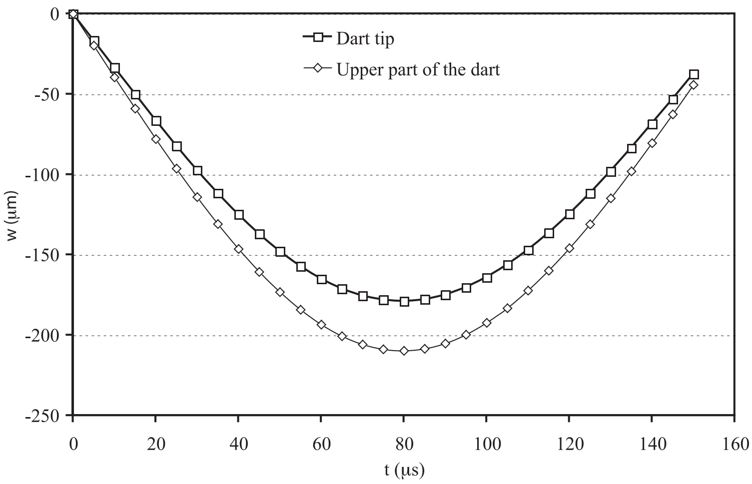

Figure 4. Displacement of the dart tip and upper part during impact.

The displacement of the dart tip and upper part during impact has been plotted in Figure 4. Initially, at impact commencement, both displacements are zero. As time passes, the dart descends until reaching a minimum value corresponding to the moment at which a maximum force is reached between the dart and the tile. The small difference in displacement between the dart tip and the dart upper part is due to compression of the dart during impact. As soon as maximum displacement is reached, the dart begins to rise, initiating the bounce. The calculation was concluded before the moment at which the dart separated itself from the tile surface.

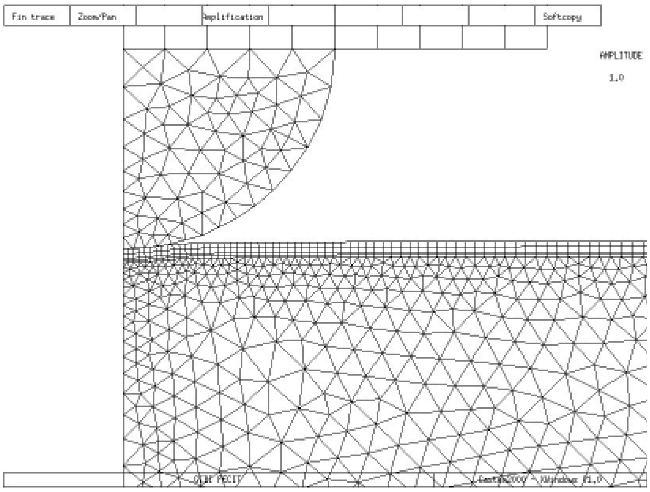

Figure 5. Displacement in the contact area at the moment of maximum strain. Dynamic calculation

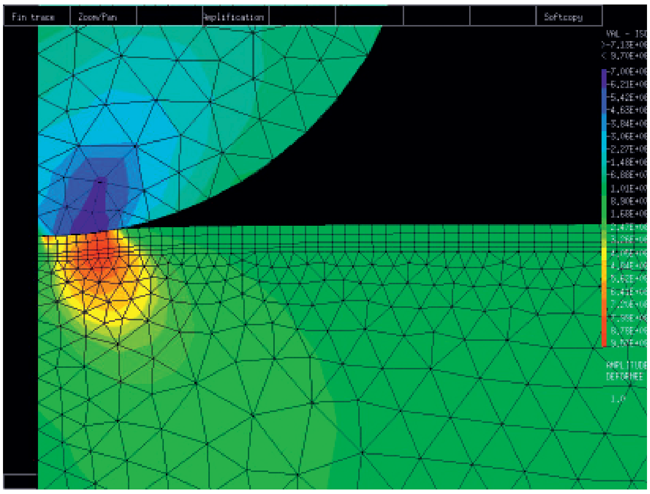

Figure 6. σ_{rz} stress at the moment of maximum strain. Dynamic calculation.

Figure 4 allows the penetration depth and impact duration (about 160 μs) to be obtained. This result is consistent with the result that may be analytically obtained, considering a homogeneous piece.

The calculation also allows tile strain (Figure 5) and stresses in the contact area to be obtained. The stress distribution contains various non-zero components (σ_{rr}, σ_{rz}, $\sigma_{\theta\theta}$,...). The shear stress (σ_{rz}) has been represented in Figure 6; the conclusions to be drawn for this component may be extended to the others. It is observed that the stresses can be very high, but they are concentrated very close to the contact point, over an area of a few tenths of a millimetre. It is precisely this small contact surface that leads to such high stresses. In some ceramic materials, compression stresses can generate plastic deformations that do not occur under any another type of stress[6].

2.2 QUASI-STATIC IMPACT

The analysis conducted previously envisages the acceleration of the dart and the piece. There is the alternative of analysing a quasi-static impact, in which the accelerations in the piece are not considered. This simplification, however, requires the introduction of information on maximum dart displacement, the force that the dart exerts on the tile, or performance of a series of static calculations with different force values, with subsequent use of the equation of conservation of mechanical energy. Quasi-static tests provide a series of advantages:

- They allow verification of the role of the accelerations. If these are not important, static experiments could be considered, which are much simpler to carry out than dynamic ones.
- The calculation time in a quasi-static test is much shorter than that in a dynamic test.
- Dynamic calculation involves resolving equations in which accelerations occur (second derivatives of the displacements), which may lead to problems in the calculation (oscillating solutions or lack of convergence).

2.2.1. Results of the simulation

In the study of quasi-static impact the same parameters were used for the dart, the tile, and the fixing layer that had been used for dynamic impact, while the same dart displacement was used as the maximum displacement calculated with the dynamic model (Figure 4).

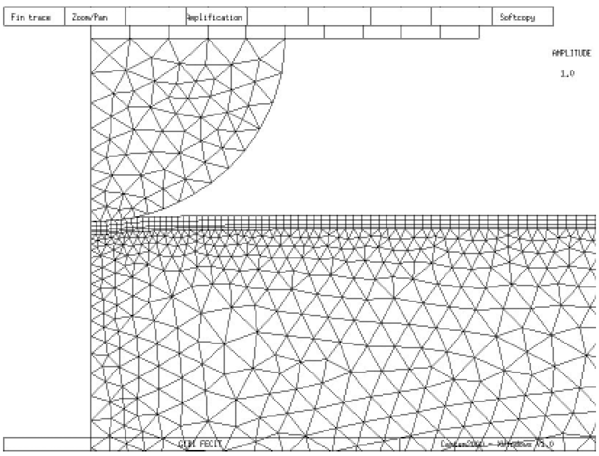

Figure 7. Displacements in the contact area at the moment of maximum strain. Quasi-static calculation.

Figure 7 shows the displacements obtained and Figure 8 displays the stresses. These figures are very similar to those obtained in the dynamic tests (Figure 5 and Figure 6). The maximum shear stress value found was 860 MPa, whereas a value of 960 MPa was obtained in the dynamic calculation. The results indicate, therefore, that the stresses were only a little higher in the dynamic test than in the quasi-static test.

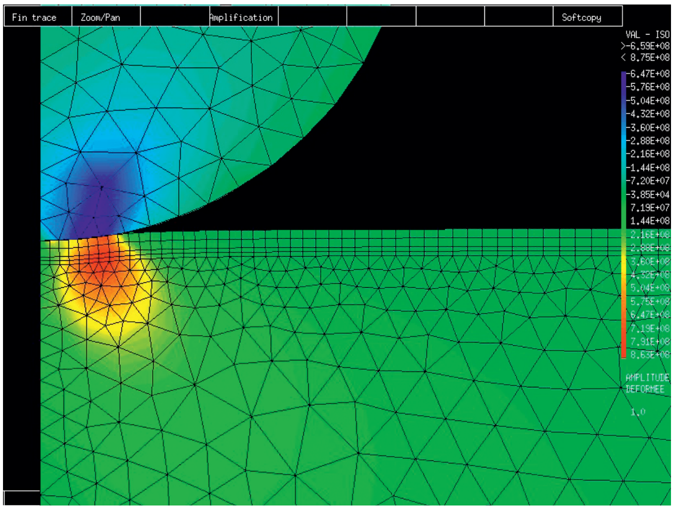

Figure 8. σ_{rz} stress at the moment of maximum strain. Quasi-static calculation.

2.2.2. *Experimental comparison between dynamic and quasi-static tests*

In order to verify the equivalence between the quasi-static and the dynamic tests, experiments were conducted with an impact pendulum[7] fitted with a load cell that recorded the force that developed during impact (Figure 9), using a dart with a 3 mm tip curvature radius, carrying out impacts on a red-body stoneware tile glazed with a porcelain tile glaze, recording the force curve as a function of time. This curve served to obtain the maximum force.

The same tip was then set in an adapter in order to perform the test in static conditions, applying the maximum force measured in the dynamic tests. Figure 10 presents an example of the results obtained. It may be observed that, for a given maximum load level, the damage produced is similar in the quasi-static and the dynamic test, corroborating the theoretically obtained results.

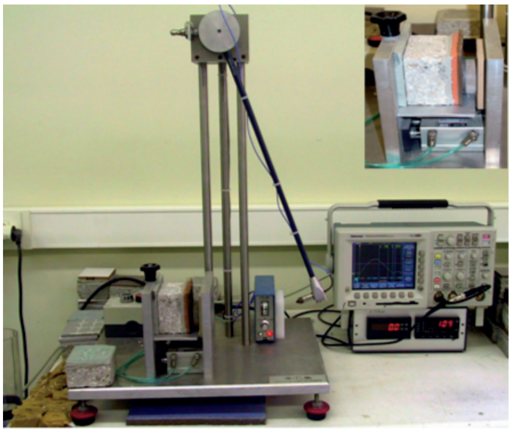

Figure 9. General view of the device used for determining impact resistance.

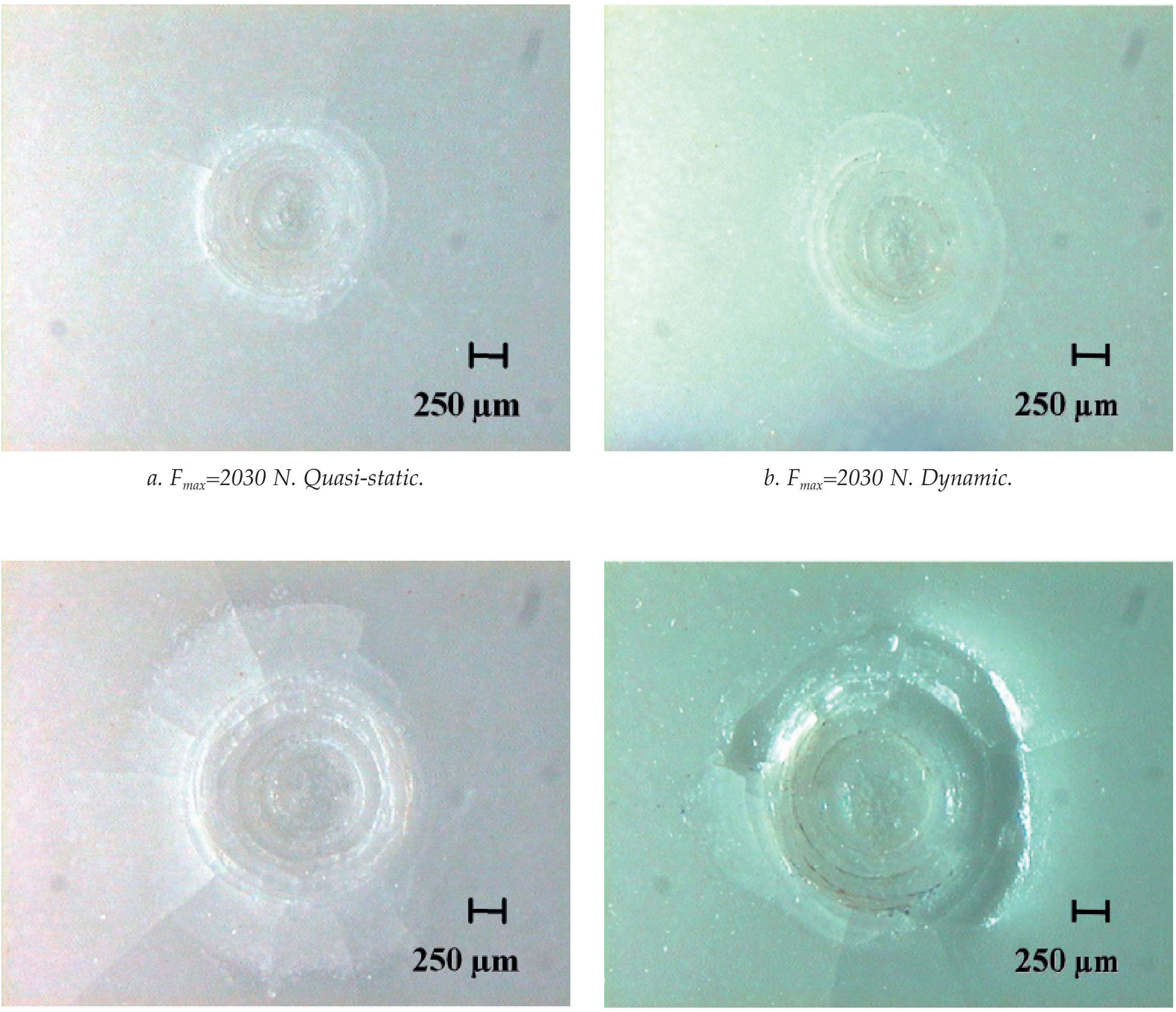

a. F_{max}=2030 N. Quasi-static.

b. F_{max}=2030 N. Dynamic.

c. F_{max}=4080 N. Quasi-static

d. F_{max}=4080 N. Dynamic

Figure 10. Appearance of the damage caused under different loads in quasi-static and dynamic impact tests.

3. PROPOSAL OF A METHOD OF QUANTIFYING IMPACT RESISTANCE

3.1. DESCRIPTION OF THE TEST

The results set out in the previous section presented the possibility of performing quasi-static tests with a view to quantifying ceramic tile impact resistance. Experiments were carried out in which cyclical loads were applied with a dart (indenter) on to a tile fixed with epoxy resin on a concrete substrate. The maximum applied load oscillated sinusoidally between a maximum value, F_{max}, and a minimum value, $F_{min} = F_{max}/10$, F_{max} being chosen as a variable. As the sinusoidal load was applied, dart displacement also changed sinusoidally. If an elastic material were involved and no fractures occurred, maximum dart displacement would take place when the force maximised and would be constant in time. In contrast, if the material suffered some type of damage, this maximum displacement could increase as the cycles were performed.

Cyclical tests with maximum forces of 2, 3, and 4 kN were carried out; for each one of these loads, the number of cycles and the oscillation frequency were varied. In order to reduce errors, 3 tests were conducted under each of the foregoing conditions.

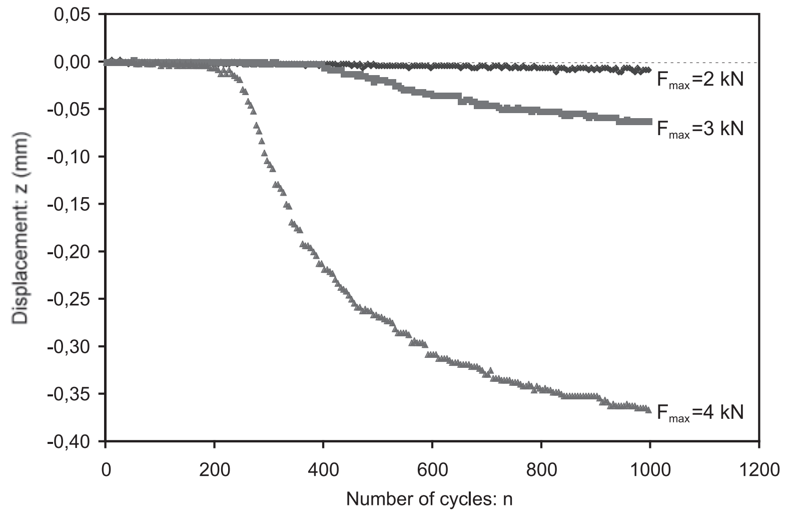

Figure 11. Penetration of the dart versus the number of cycles for different maximum loads.

Figure 11 shows the typical result of a cyclical test. In this figure the penetration of the indenter (z) has been plotted as a function of the number of cycles (n), for the three tested maximum force values. Three stages may be observed in this graph:

- *Initial stage:* in which the slope is practically constant for a given load. Material damage begins to occur.
- *Intermediate stage:* in which the slope increases very noticeably. Glaze damage is very significant.
- *Final stage:* in which the slope of z as a function of time decreases again. This decrease possibly occurs because, when damage increases, the contact surface between the dart tip and the tile is larger. This reduces the pressure in the contact area and, hence, the strength of the stress field that causes the cracks to advance.

3.2. PARAMETERISATION OF IMPACT RESISTANCE

In order to obtain quantitative information from these cyclical tests, the curves in Figure 11 were fitted to an empirical equation of the form:

$$z = z_0 - m_1 n - A(1 - m_2 n)\left(1 - e^{-(n-n_0)/\tau}\right)u(n - n_0)$$

Eq. 1

where u(x) is the unit step function, defined as:

$$u(x) = \begin{cases} 0 & \text{si} \quad x < 0 \\ 1 & \text{si} \quad x \geq 0 \end{cases}$$

z_0: Initial displacement. This does not depend on the characteristics of the material to be analysed. (mm)

m_1: Slope of the initial section of curve z(n). (mm/cycle)

m_2: Parameter related to the slope of the final section of curve z(n). (mm/cycle)

A: Difference at the ordinate of the initial straight line ($-m_1n$) and the asymptote to which z(n) tends. (mm)

n_0: Number of cycles at which the transition occurs between the initial and the intermediate stage.

b: Parameter quantifying the rapidity (expressed in number of cycles) of the transition between the middle and the end section. When b increases, the transition occurs more slowly.

The physical meanings of the constants z_0, m_1, m_2, A, n_0, and b are displayed graphically in Figure 12.

The parameter that correlates most closely with impact resistance is m_1, which is the parameter that controls the beginning of the damage that occurs in the tile. When the intermediate stage is reached, the damage is already too high.

4. FACTORS THAT INFLUENCE IMPACT RESISTANCE

4.1. TILE FIXING (INSTALLATION)

4.1.1. Results of the simulation

With a view to analysing the stresses that develop during impact under deficient fixing conditions, a simulation was conducted by finite elements, using the geometry indicated in section 2.1.2, and considering an applied load of 3 kN. Figure 13 shows the meshes used to simulate correct and deficient fixing. Deficient fixing was simulated by creating a cylindrical void, 20 mm in diameter, beneath the tile on the vertical of the dart

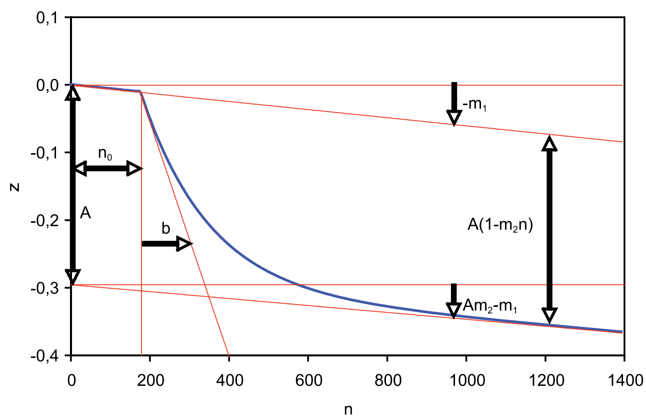

Figure 12. Geometric meaning of the parameters of Eq. 1.

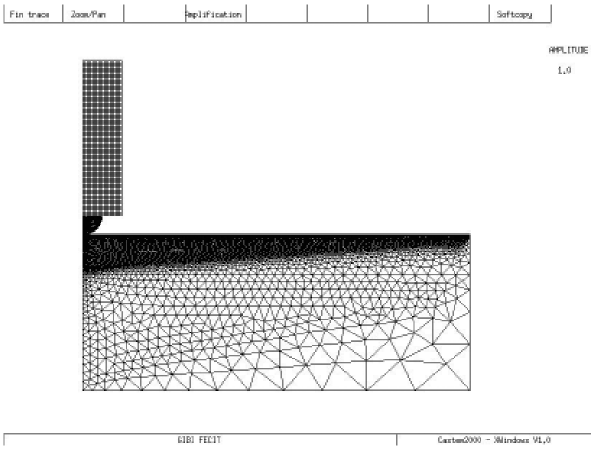

a. Mesh with correct fixing.

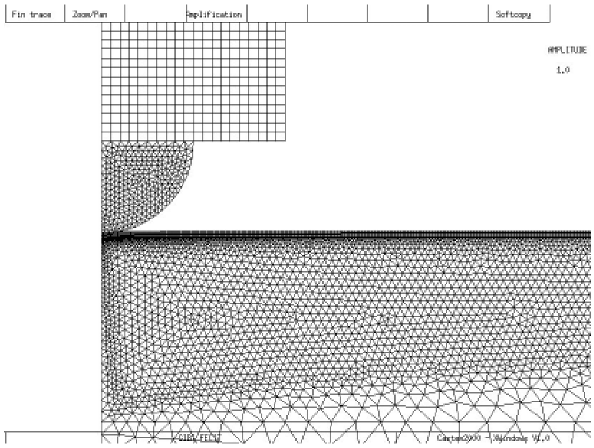

b. Detail of the correct fixing mesh.

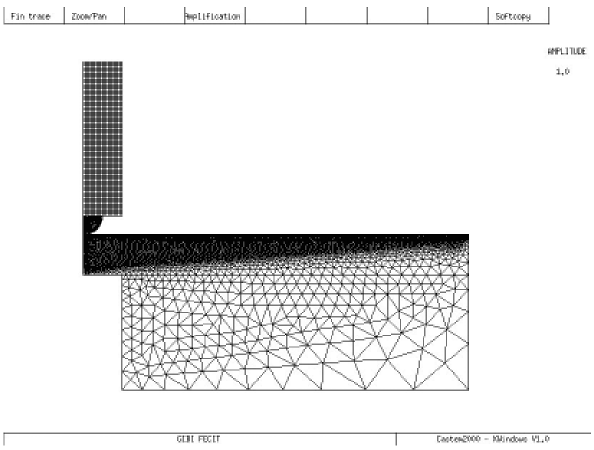

c. Mesh with deficient fixing.

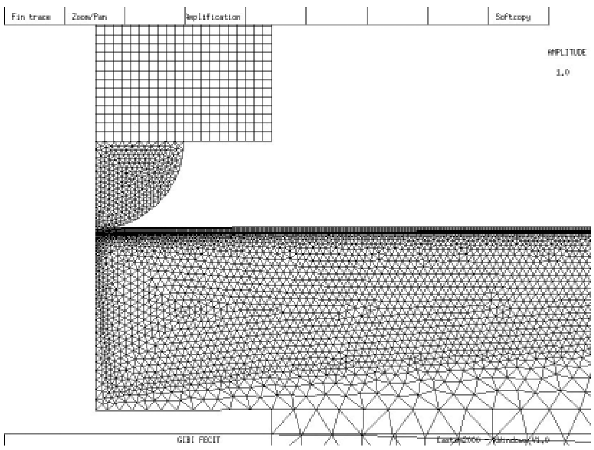

d. Detail of the deficient fixing mesh.

Figure 13. Mesh made to calculate the effect of correct fixing (a and b) and deficient fixing (c and d).

When the load is applied, the stress profile in the tile in the dart contact area is very similar in both cases (correct and deficient fixing). The greatest changes in the stress profile occur in the lower part of the substrate. Figure 14 shows the residual stress in the case of a correct tile installation, where the maximum stress value is 5 MPa. In contrast, Figure 15 displays the stress profile in the case of deficient fixing. This figure clearly evidences a very high concentrated tensile stress in the lower part of the piece; here the stress reaches 22 MPa, i.e. more than 4 times the value it would have with proper fixing. If a larger force were applied, this stress could lead to tile failure caused by bending. In this last situation, the type of the fracture would be very different: there would be no spalling, but cracking of the tile.

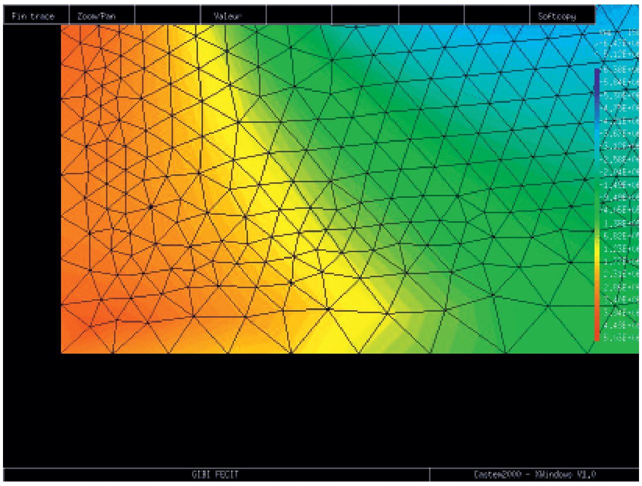

Figure 14. σ_{rr} stress in the lower part of the substrate. Correct fixing.

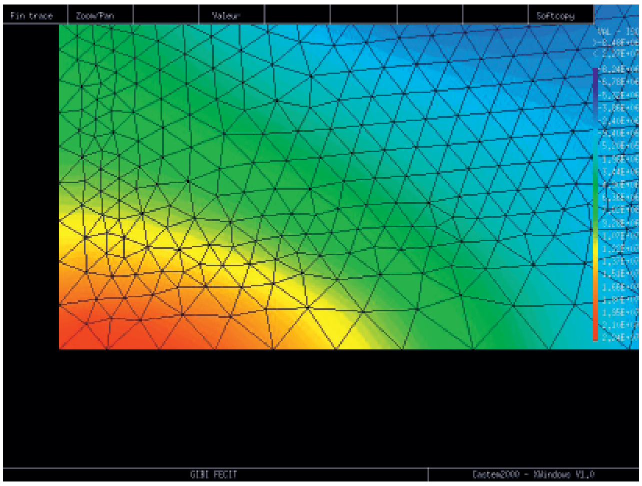

Figure 15. σ_{rr} stress in the lower part of the substrate. Deficient fixing.

4.1.2. Laboratory tests to reproduce deficient fixing

In order to verify the effect of deficient fixing under laboratory conditions, a tile was set on a nylon washer (Figure 16) and a force was then applied by means of the dart, such that the dart was aligned with the centre of the washer. The results obtained (Figure 17) show that, though the dart generated a light track, no spalling occurred; instead the tile broke.

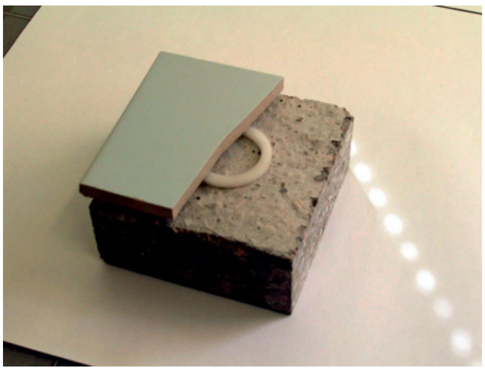

Figure 16. Assembly used to simulate deficient fixing.

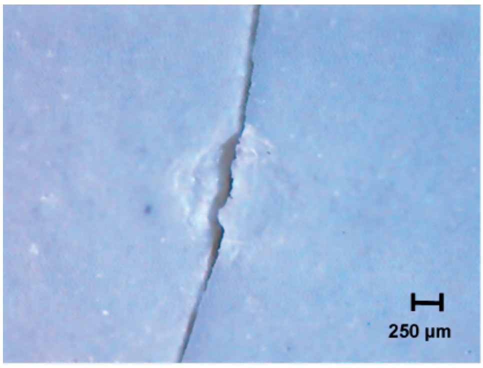

Figure 17. Appearance of the fracture with deficient fixing.

4.2. NATURE OF THE ENGOBE AND THE GLAZE

In order to establish the effect of the engobe and the glaze on impact resistance, tests were designed, under industrial conditions, in which the type of engobe and glaze was varied. The tiles were fixed with epoxy resin on a concrete base and their impact resistance was determined using parameter m_1 of Eq. 1. Table 1 presents the results of the test pieces in which two types of engobe (standard and refractory) were used.

It may be observed that the tiles containing the refractory engobe displayed a higher value of m_1. This might be because greater refractoriness could lead to a smaller modulus of elasticity and greater deformability of the engobe, which would in turn increase the stresses in glaze.

Reference	Substrate	Engobe	Glaze	Firing curve	m_1 (nm/cycle)
T1	Porcelain tile	Standard porcelain	Matt porcelain	Porcelain tile	51 ± 10
T2	Porcelain tile	Refractory porcelain	Matt porcelain	Porcelain tile	158 ± 16

Table 1. Characteristics of the tested industrial tiles.

Table 2 presents the results obtained when the type of glaze was varied. It shows that, despite using two types of quite different glazes, the impact resistance was practically the same.

Reference	Substrate	Engobe	Glaze	Firing curve	m_1 (nm/cycle)
T3	Porcelain tile	Stoneware	Glossy stoneware	Stoneware	215 ± 18
T4	Porcelain tile	Stoneware	Matt stoneware	Stoneware	200 ± 17

Table 2. Characteristics of the tested industrial tiles.

4.3. NATURE OF THE SUBSTRATE

In order to analyse the effect of the substrate, the tiles indicated in Table 3 were prepared, in which the type of substrate (stoneware/porcelain tile) and the firing curve were varied. In the case of the tiles fired with the porcelain tile curve it was necessary to place the tiles on a refractory slab. Table 3 also lists the modulus of elasticity (E), mechanical strength (σ_R), and parameter m_1.

It may be observed that there are no large differences between the value of m_1 for the stoneware and the porcelain tiles fired with the same temperature curve. When these materials, each fired according to its corresponding curve, are compared, porcelain tile is observed to perform better in relation to impact.

There is a parallelism between the mechanical properties (E, σ_R) and impact resistance, quantified as m_1. In Figure 18, m_1 has been plotted as a function of E; the plot shows that m_1 decreases as E increases (impact resistance diminishes).

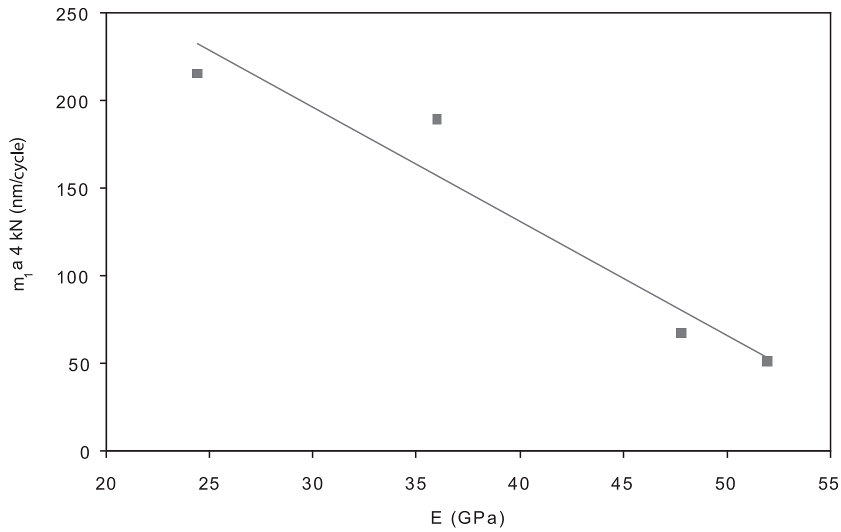

Figure 18. Evolution of parameter m_1 as a function of the modulus of elasticity.

Reference	Substrate	Glaze	Firing curve	E (GPa)	σ_R (MPa)	m_1 (nm/cycle)
T5	Stoneware	Glossy stoneware	Stoneware	36.0 ± 1.2	36.7 ± 1.7	189 ± 38
T3	Porcelain tile	Glossy stoneware	Stoneware	24.4 ± 0.6	27.7 ± 1.2	215 ± 18
T6	Stoneware	Matt porcelain	Porcelain tile on refractory slab	47.8 ± 1.5	45.2 ± 1.9	67 ± 10
T1	Porcelain tile	Matt porcelain	Porcelain tile	52.0 ± 1.0	52.4 ± 1.7	51 ± 10

Table 3. Characteristics of the tested industrial tiles.

5. CONCLUSIONS

- It has been verified that very high stress develops during impact, which is also highly concentrated in the proximities of the impact point.

- The results of the simulations indicate that the impact of an object on a tile does not involve important accelerations in the piece. This allows impact to be considered as a quasi-static process. This result has been verified under laboratory conditions.

- A method has been developed that allows the impact resistance of a ceramic tile to be quantified. The method is based on determining the deterioration that a tile undergoes as a result of the application of a cyclical load, and leads to a parameter m_1 that quantifies this deterioration.

- The existence of deficient fixing leads to tile failure, without any significant spalling appearing. The calculations conducted indicate that rupture occurs because very significant tensile stress develops in the lower part of the tile.

- The use of more or less refractory engobes has an important influence on impact resistance. When refractoriness increases, impact resistance decreases, possibly owing to a decrease in the modulus of elasticity.

- The nature of the glaze has little influence on impact resistance.

- The substrate plays a very important role in impact resistance. In general, substrates with higher moduli of elasticity perform better under impact. This is because when the modulus of elasticity increases, strain in the glaze decreases, reducing the shear and tensile stresses.

REFERENCES

[1] UNE-EN ISO 10545-5. Baldosas cerámicas - Determinación de la resistencia al impacto por medición del coeficiente de restitución.

[2] SILVA, G et al. Development of a new method of evaluating impact resistance. Key Eng. Mater., 206-213, 1815-1818, 2002.

[3] MARCO, J. et at. Aplicación de la acelerometría a la medida de propiedades mecánicas de materiales. Téc. Cerám., 303, 621-635, 2002.

[4] BEAKE, B.D. et al. Micro-impact testing: a new technique for investigating fracture toughness. Thin Solid Films, 398-399, 438-443, 2001.

[5] Code Aster. http://www.code-aster.org [Consulta: 2007-09-27).

[6] FISHER-CRIPPS, A.C. Stress Analysis of contact deformation in quasi-plastic ceramics. J. Am. Ceram. Soc, 79 (10), 2609-2618, 1996.

[7] SILVA MORENO, G. Estudio experimental de la durabilidad de baldosas cerámicas: resistencia al impacto y a la abrasión. Castellón: UJI, 2005. [Tesis Doctoral]